Supporting Information for

Reusable Cyanide Sensing via Activation of C-H Group: Trifluoromethylcarbinol-directed *meta*-C-H Cyanomethylation of Naphthalimide

Yayun Chen, Xiaoxue Hu, Caihui Rao, Zheyao Li, Lu Chen, Chao Fu and Chuanxiang Liu *

School of Chemical and Environmental Engineering, Shanghai Institute of Technology, Shanghai 201418, China

E-mail: cxliu@sit.edu.cn

Contents of Supporting Information

1. ^{1}H-NMR, ^{13}C-NMR, ^{19}F-NMR and HRMS-ESI spectrum of 2a

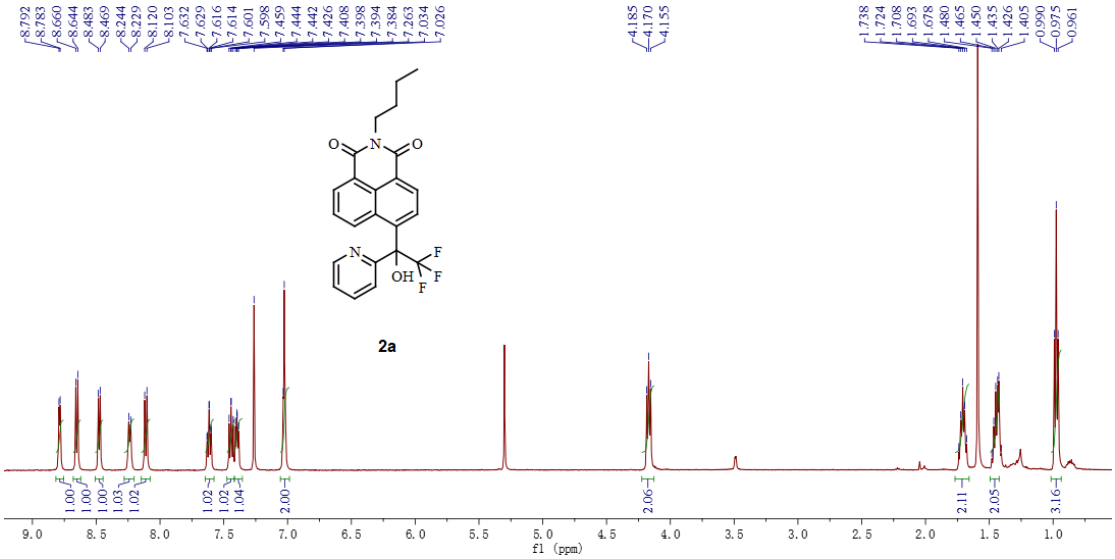

Figure S1. ^{1}H-NMR ($CDCl_3$, 500 MHz) spectrum of compound **2a**

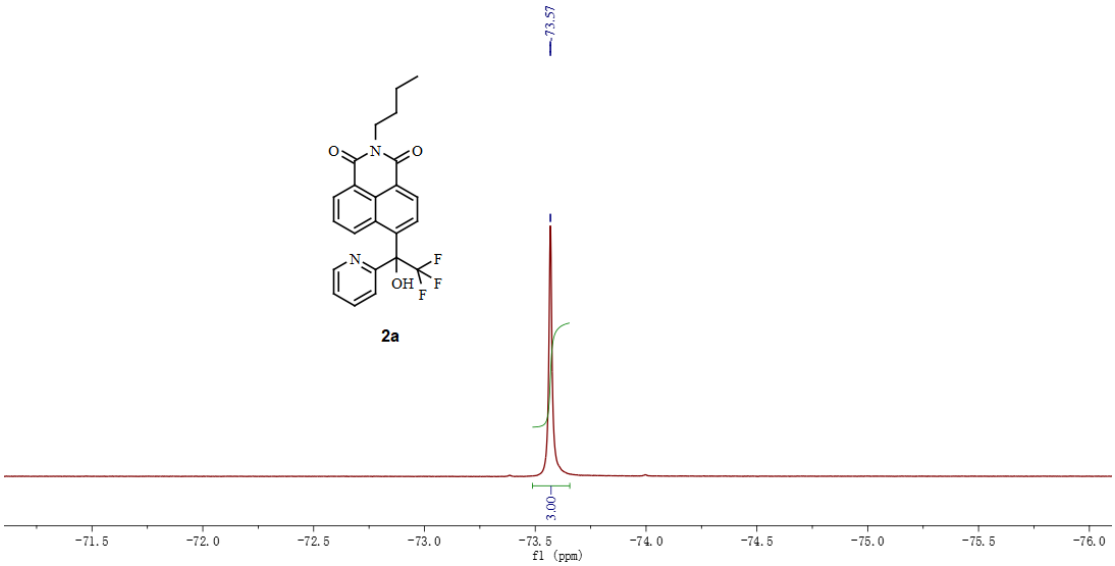

Figure S2. ^{19}F-NMR ($CDCl_3$, 470 MHz) spectrum of compound **2a**

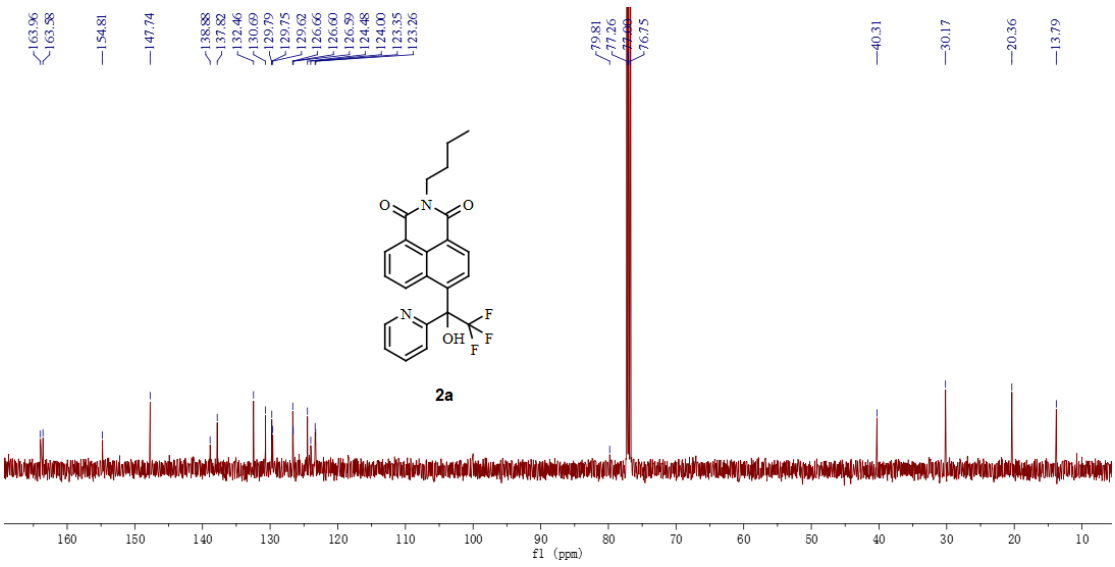

Figure S3. ^{13}C-NMR ($CDCl_3$, 125 MHz) spectrum of compound **2a**

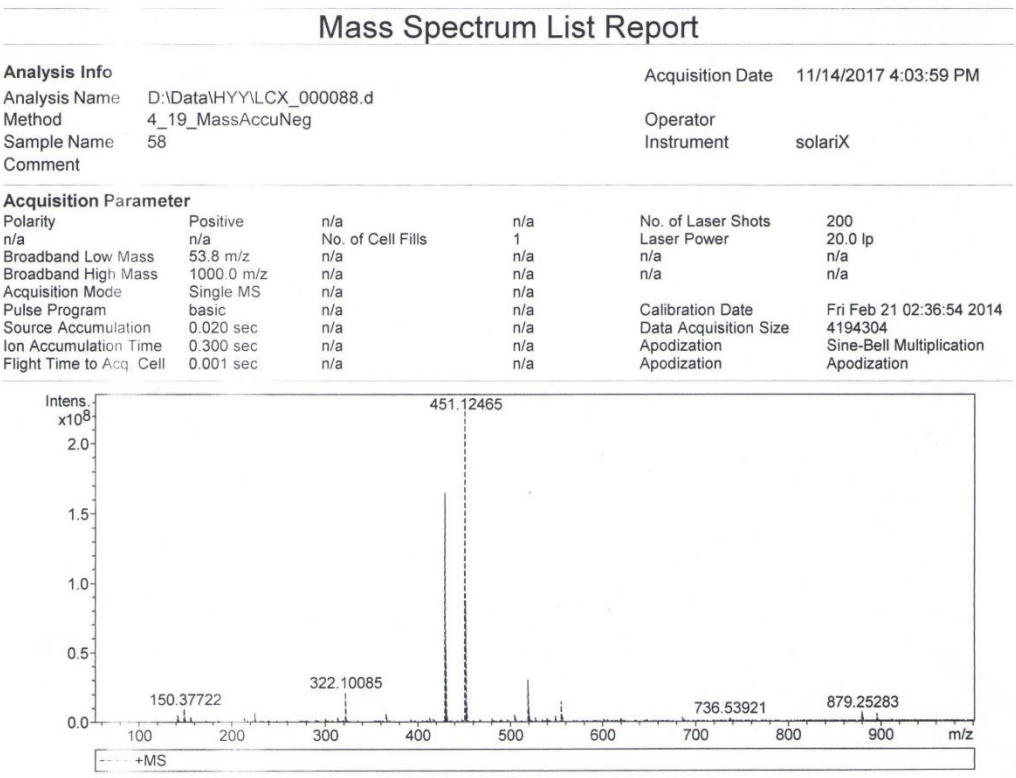

Figure S4. HRMS-ESI mass spectrum of compound **2a**

2. ^{1}H-NMR, ^{13}C-NMR and ^{19}F-NMR spectrum of the mixture of isomers 3

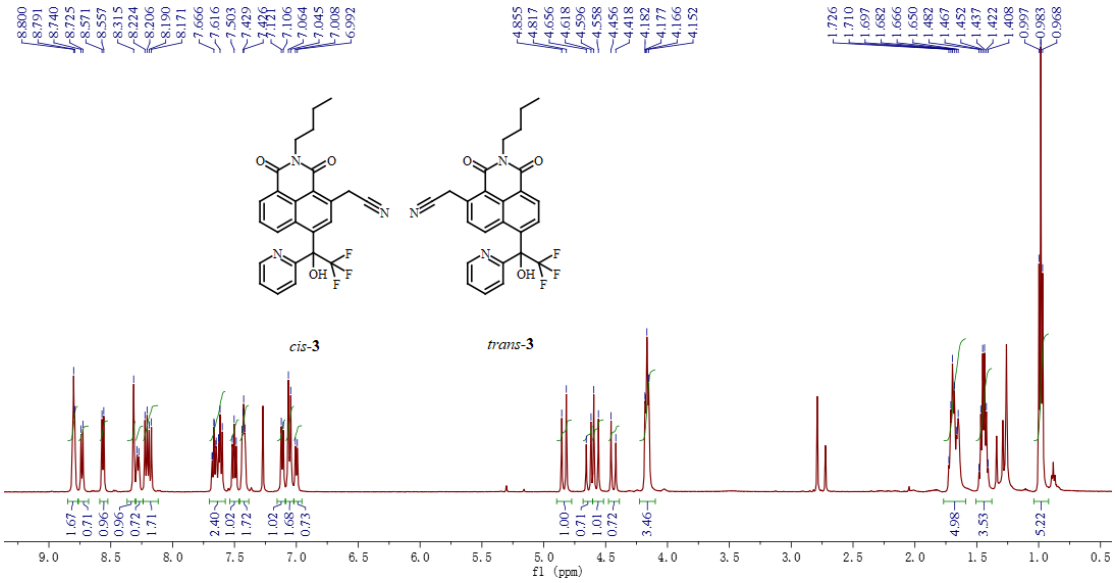

Figure S5. ^{1}H-NMR ($CDCl_3$, 500 MHz) spectrum of the mixture of *cis*-**3** and *trans*-**3** (1:0.7)

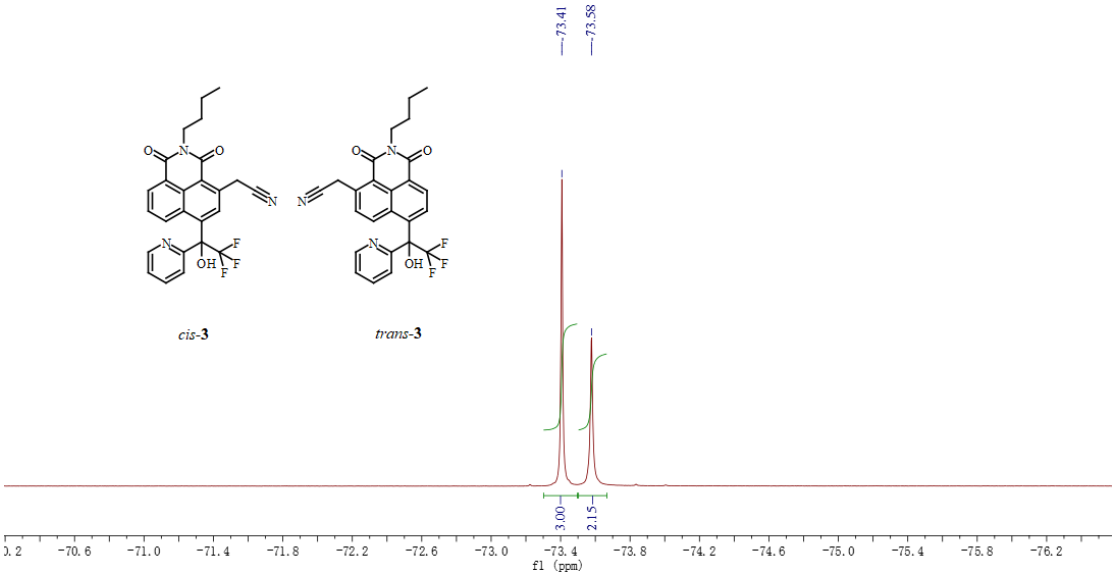

Figure S6. ^{19}F-NMR ($CDCl_3$, 470 MHz) spectrum of the mixture of *cis*-**3** and *trans*-**3** (1:0.7)

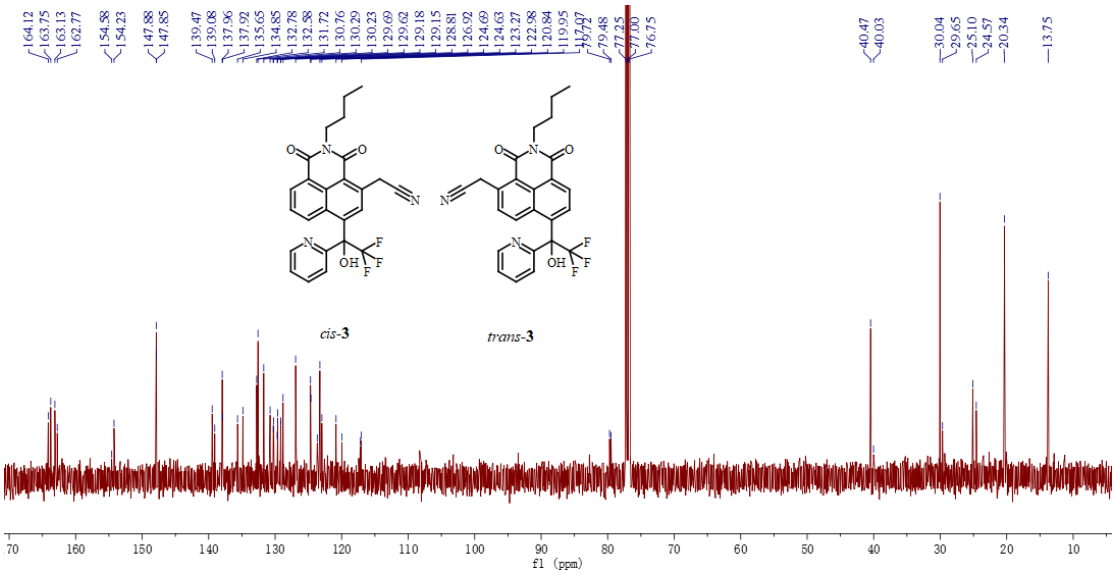

Figure S7. ^{13}C-NMR ($CDCl_3$, 125 MHz) spectrum of the mixture of *cis*-**3** and *trans*-**3** (1:0.7)

3. ^{1}H-NMR, ^{13}C-NMR, ^{19}F-NMR and HRMS-ESI spectrum of *cis*-3 and *trans*-3

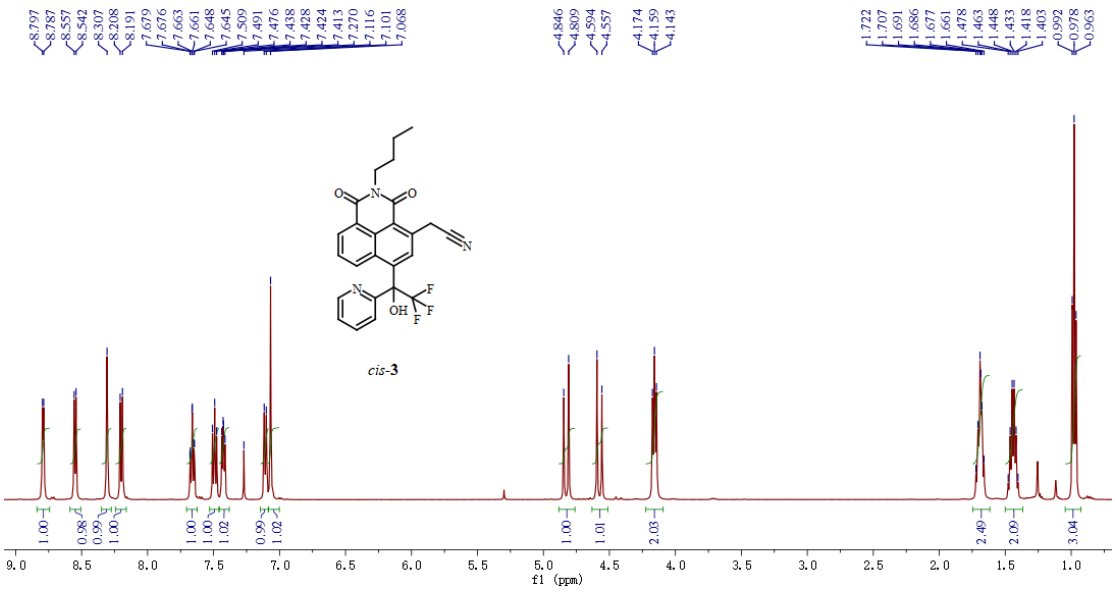

Figure S8. ^{1}H-NMR ($CDCl_3$, 500 MHz) spectrum of compound *cis*-**3**

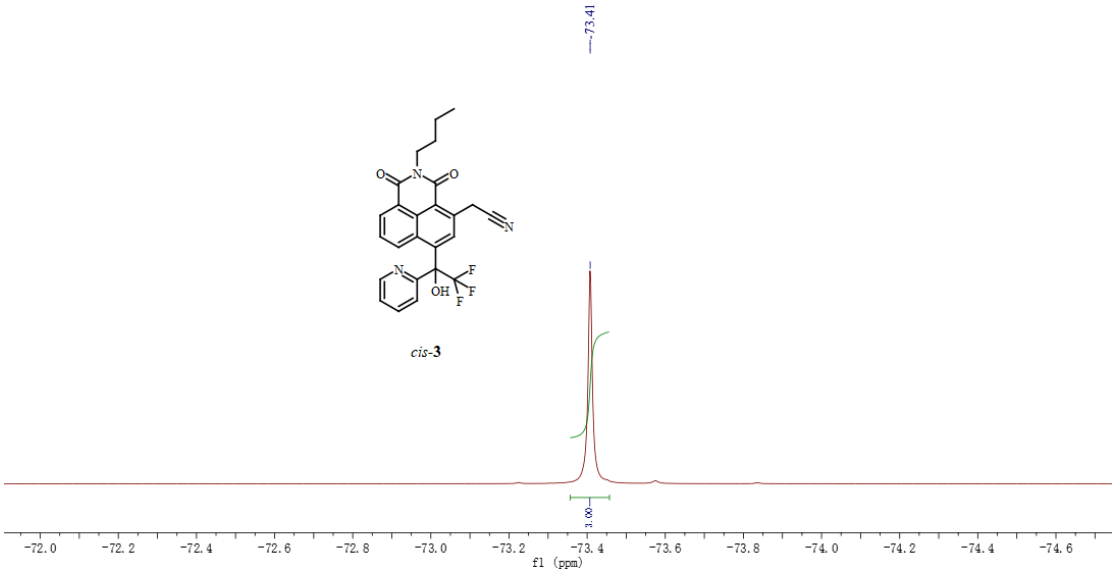

Figure S9. ^{19}F-NMR ($CDCl_3$, 470 MHz) spectrum of compound *cis*-**3**

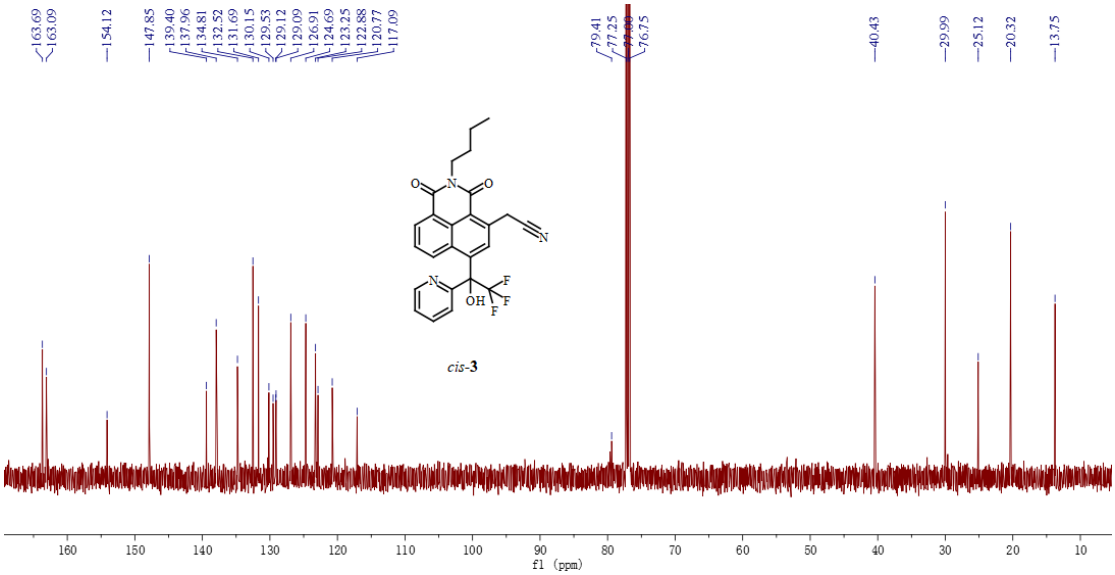

Figure S10. ^{13}C-NMR ($CDCl_3$, 125 MHz) spectrum of compound *cis*-**3**

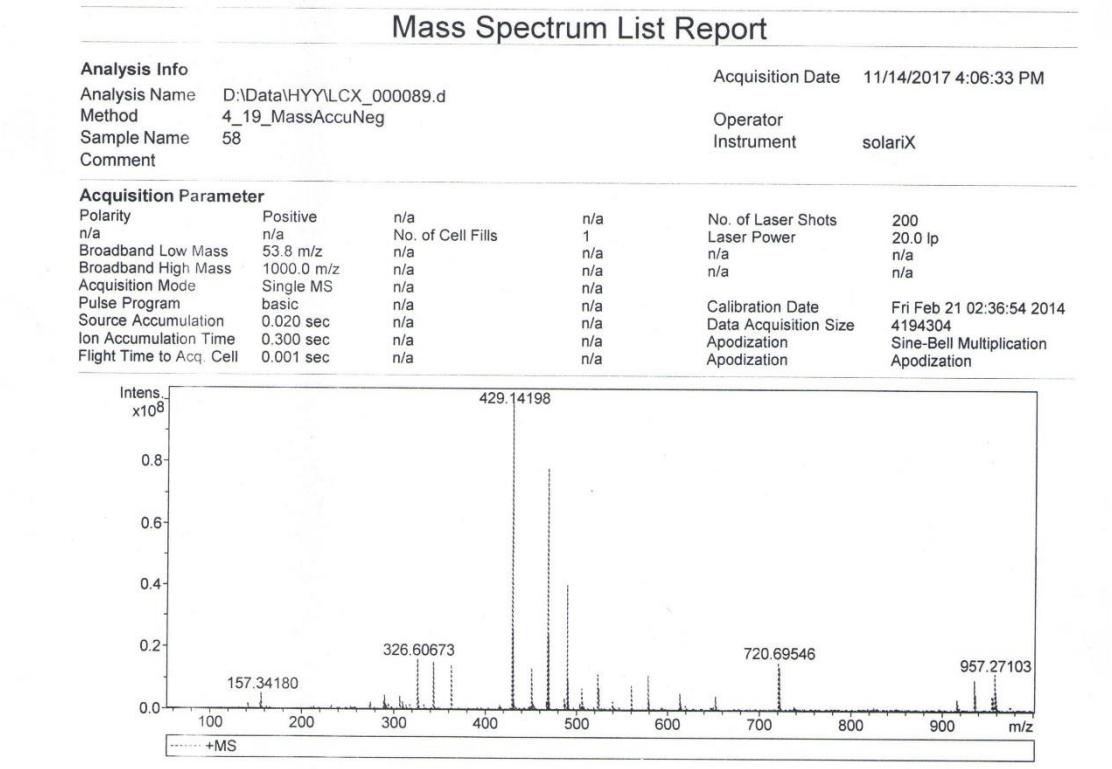

Figure S11. HRMS-ESI mass spectrum of compound *cis*-**3**

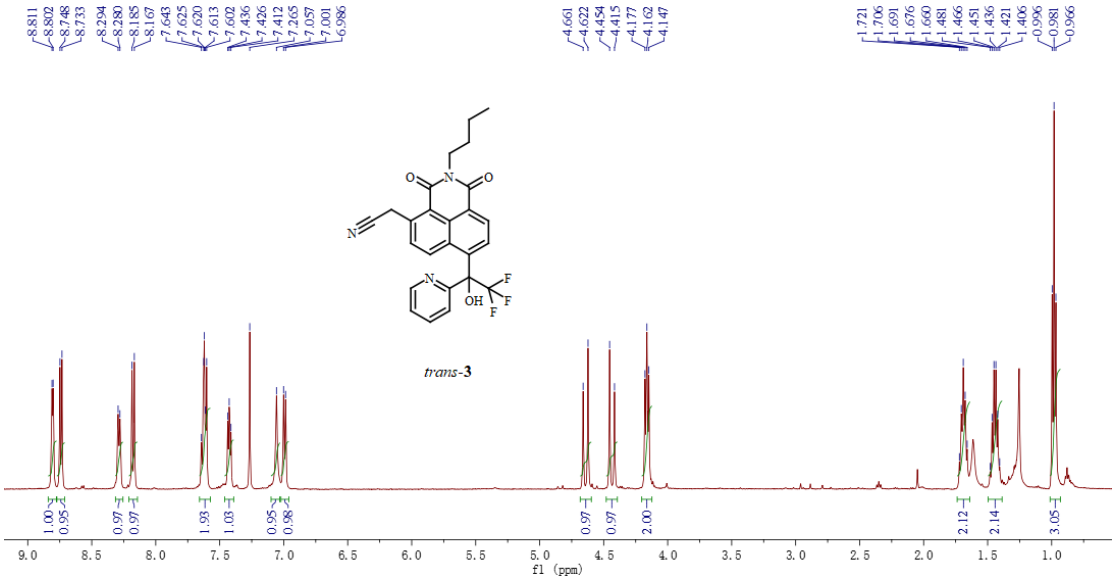

Figure S12. ^{1}H-NMR ($CDCl_3$, 500 MHz) spectrum of compound *trans*-**3**

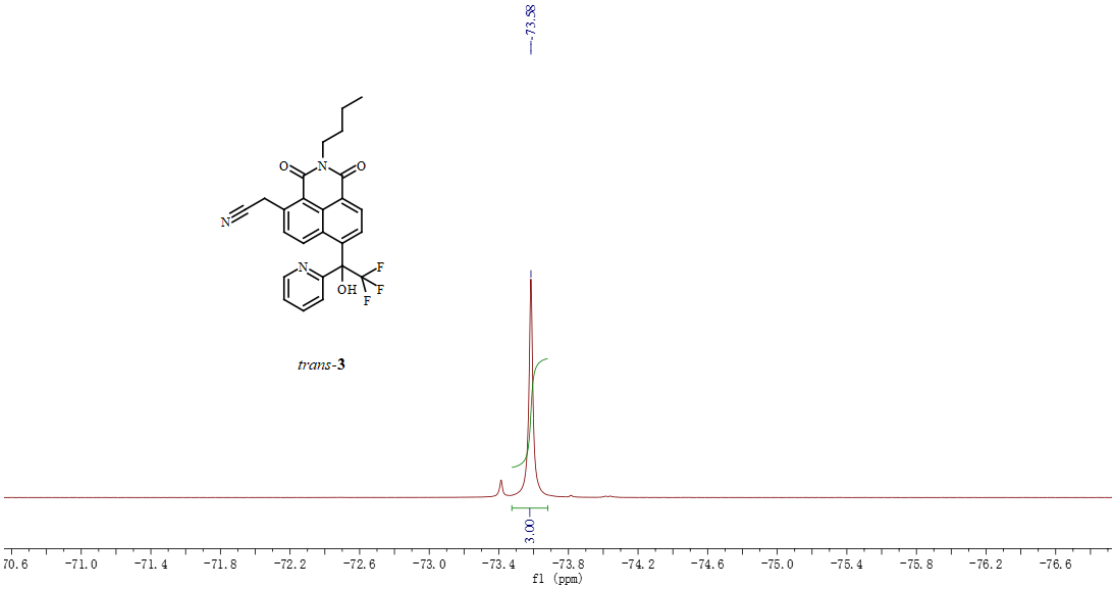

Figure S13. ^{19}F-NMR ($CDCl_3$, 470 MHz) spectrum of compound *trans*-**3**

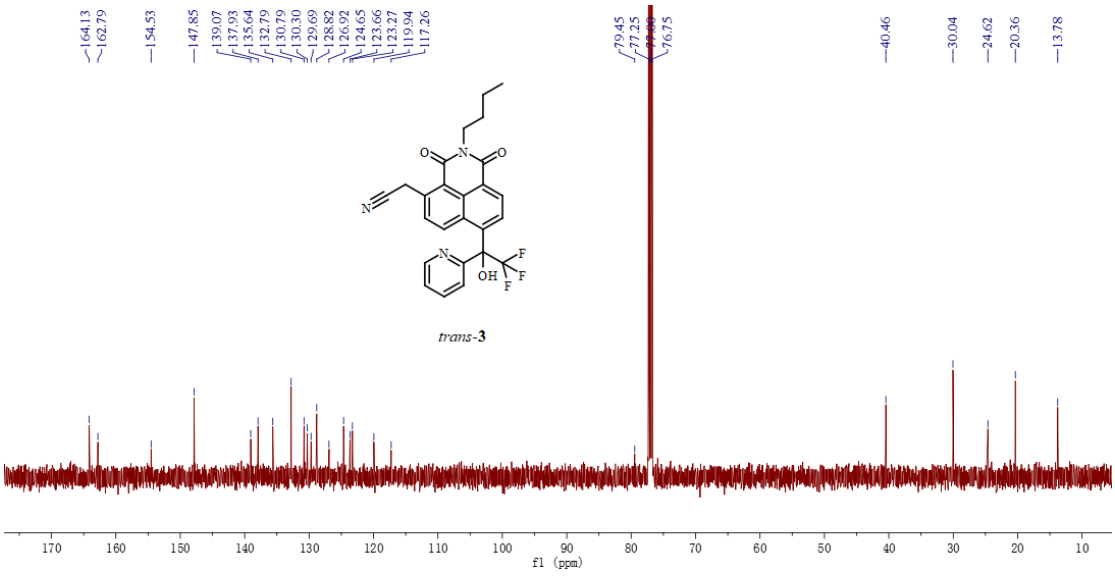

Figure S14. ^{13}C-NMR ($CDCl_3$, 125 MHz) spectrum of compound *trans*-**3**

Mass Spectrum List Report

Analysis Info

Analysis Name	D:\Data\HYY\LCX_000106.d	Acquisition Date	1/11/2018 12:31:58 PM
Method	4_19_MassAccuNeg	Operator	
Sample Name	58	Instrument	solariX
Comment			

Acquisition Parameter

Polarity	Positive	n/a	n/a	No. of Laser Shots	200
n/a	n/a	No. of Cell Fills	1	Laser Power	20.0 lp
Broadband Low Mass	53.8 m/z	n/a	n/a	n/a	n/a
Broadband High Mass	1000.0 m/z	n/a	n/a	n/a	n/a
Acquisition Mode	Single MS	n/a	n/a		
Pulse Program	basic	n/a	n/a	Calibration Date	Fri Feb 21 02:36:54 2014
Source Accumulation	0.020 sec	n/a	n/a	Data Acquisition Size	4194304
Ion Accumulation Time	0.500 sec	n/a	n/a	Apodization	Sine-Bell Multiplication
Flight Time to Acq. Cell	0.001 sec	n/a	n/a	Apodization	Apodization

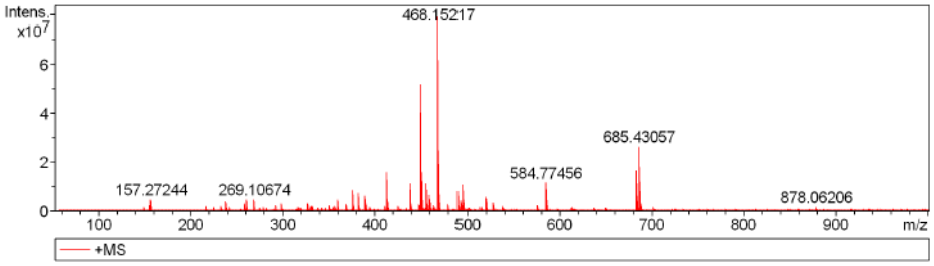

Figure S15. HRMS-ESI mass spectrum of compound *trans*-**3**

4. ^{1}H-NMR, ^{13}C-NMR, ^{19}F-NMR and HRMS-ESI spectrum of 2b and 4

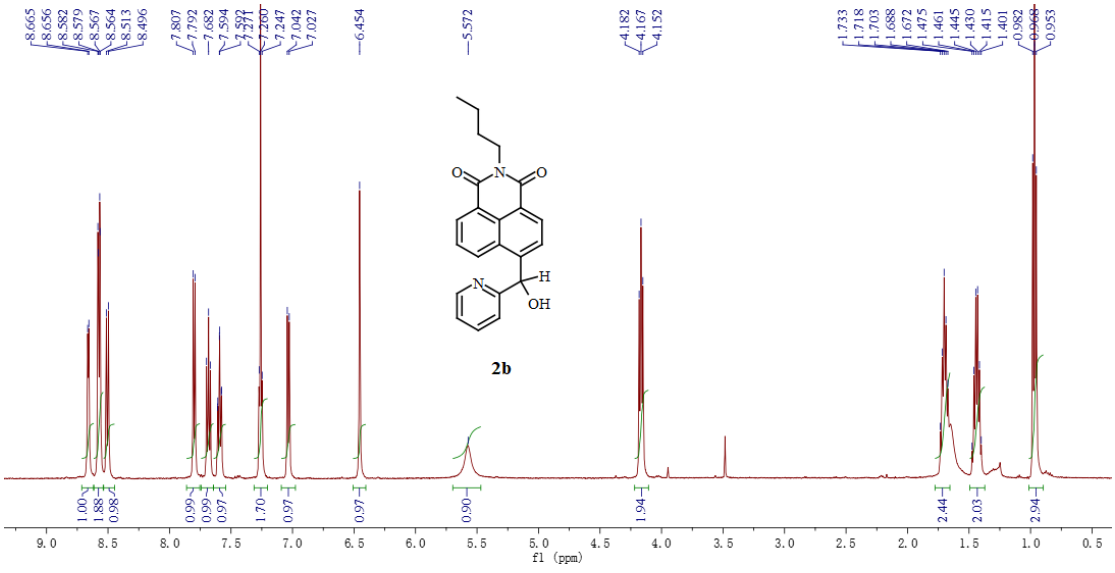

Figure S16. ^{1}H-NMR ($CDCl_3$, 500 MHz) spectrum of compound **2b**

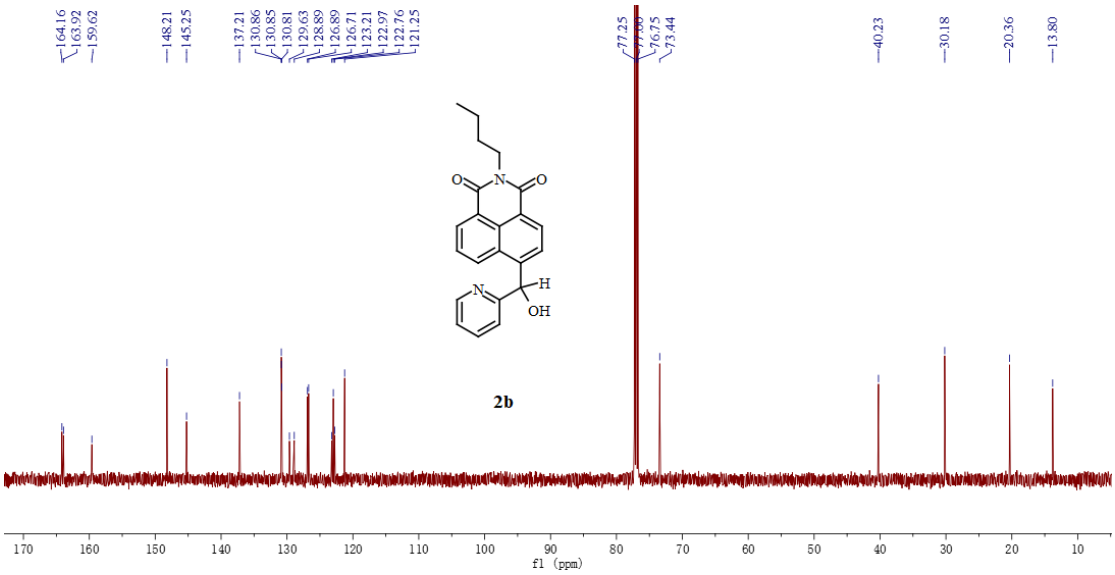

Figure S17. ^{13}C-NMR ($CDCl_3$, 125 MHz) spectrum of compound **2b**

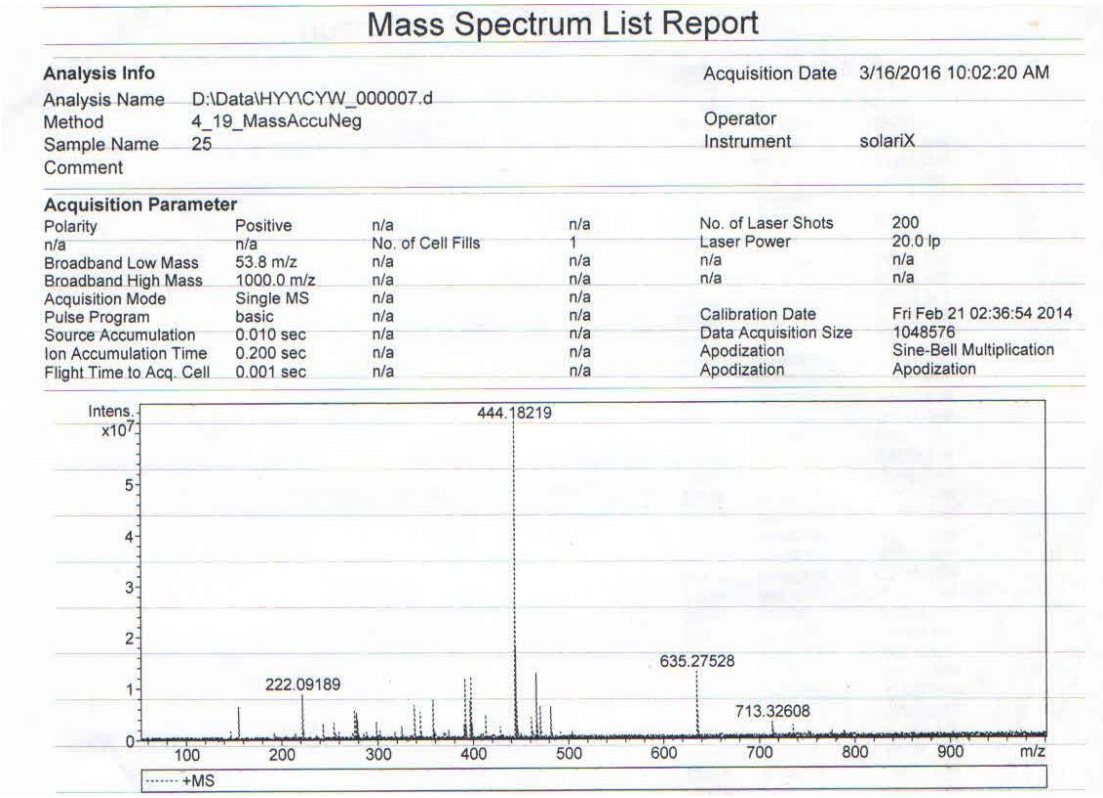

Figure S18. HRMS-ESI mass spectrum of compound **2b**

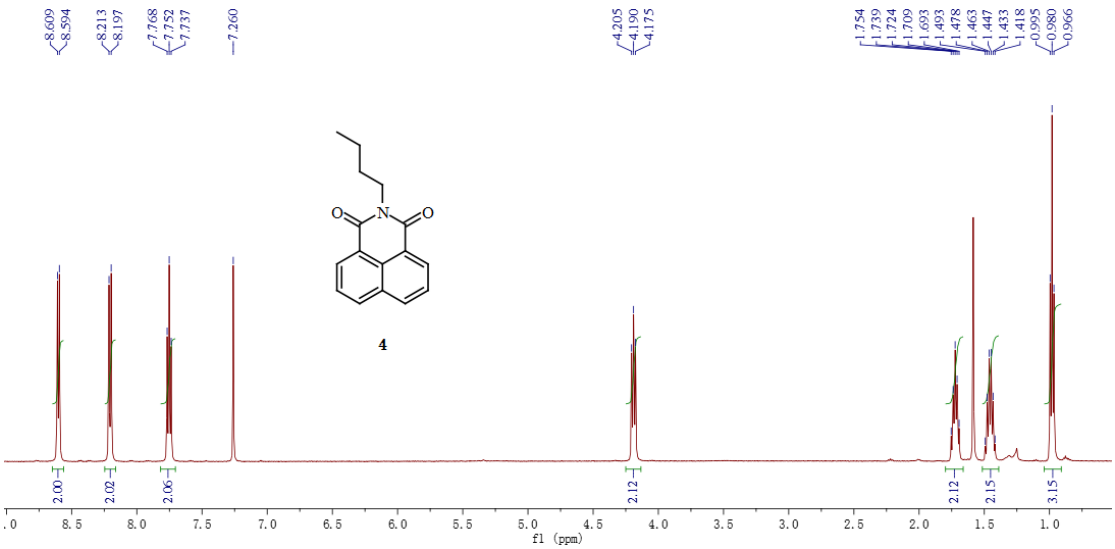

Figure S19. ^{1}H-NMR ($CDCl_3$, 500 MHz) spectrum of compound **4**

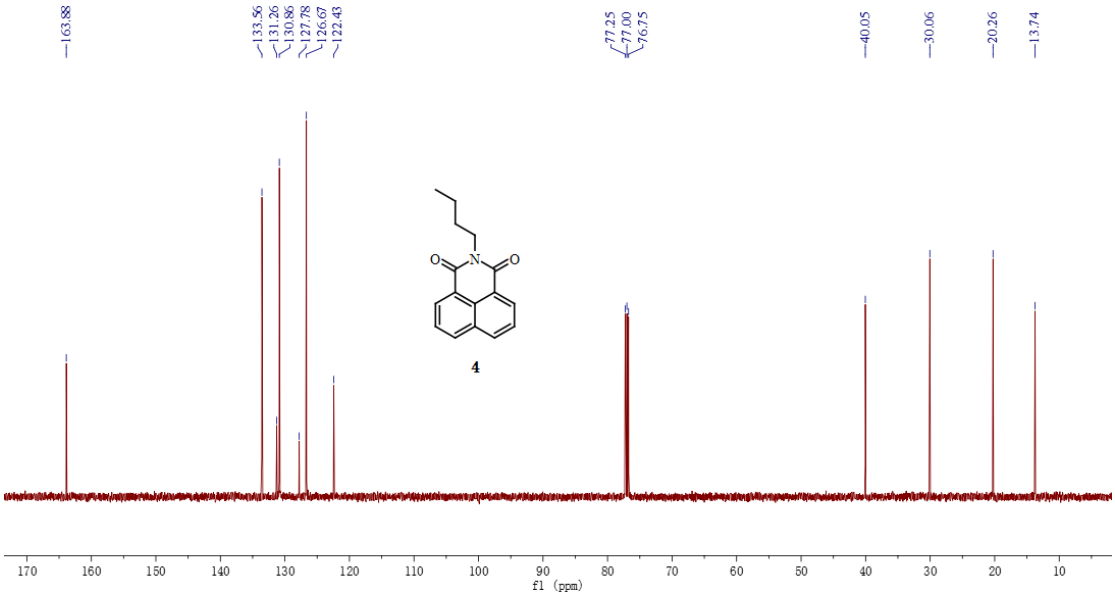

Figure S20. ^{13}C-NMR ($CDCl_3$, 125 MHz) spectrum of compound **4**

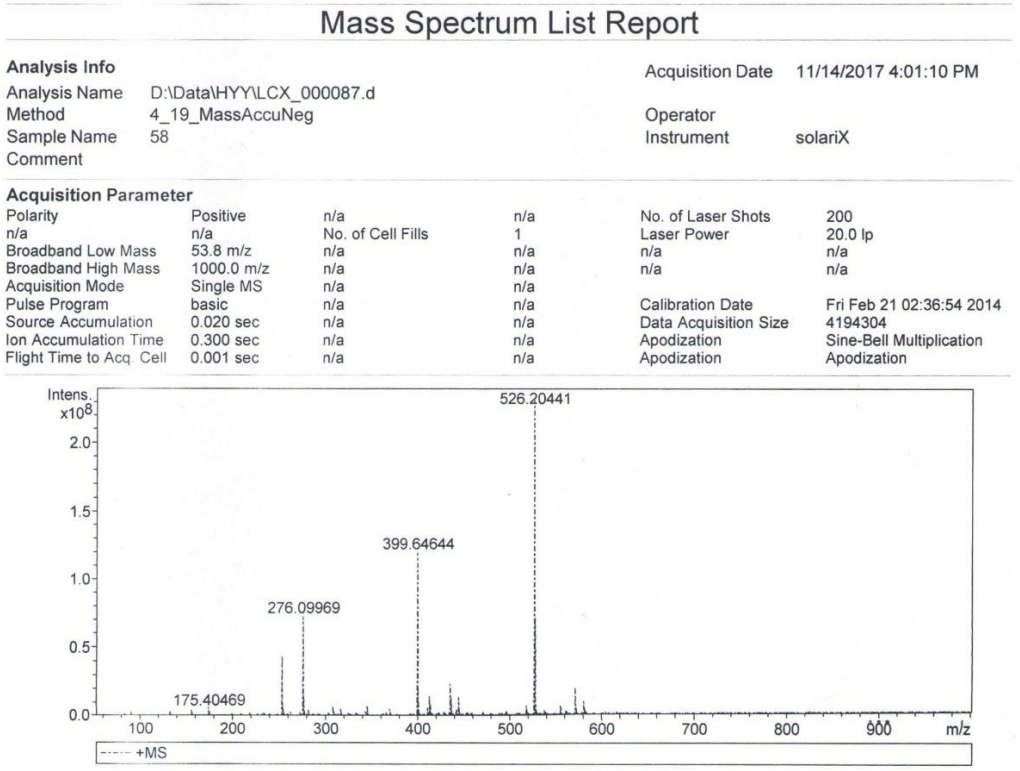

Figure S21. HRMS-ESI mass spectrum of compound **4**

5. Molecular modeling calculations for 2a, *cis*-3, deprotonation of *cis*-3

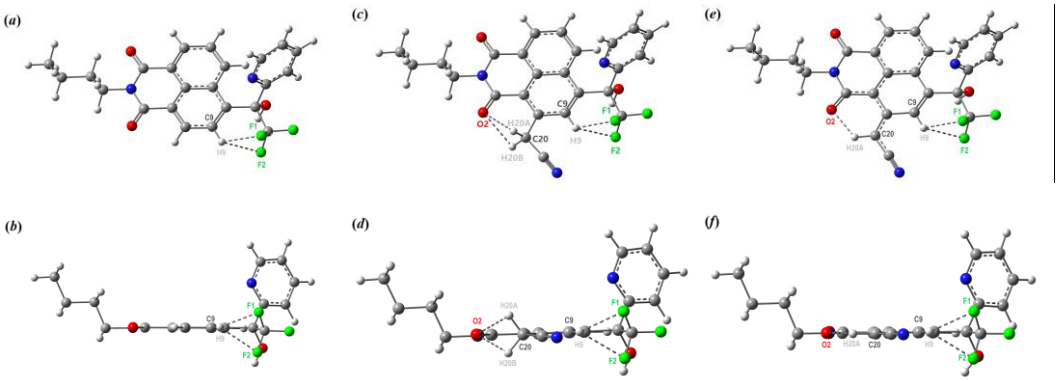

	Bond lengths				angles			
	H9-F1	H9-F2	O2/O1-H20A	O2/O1-H20B	C9-H9-F1	C9-H9-F2	C20-H20A-O2	C20-H20B-O2
2	2.26178	2.44729			118.90694	108.53560		
cis-**3**	2.25124	2.42559	2.42615	2.34624	119.41000	110.06837	90.56082	94.87512
Deprotonation of cis-**3**	2.29849	2.40999	2.06244		118.77955	111.46043	122.21220	

Figure S22. Equilibrium structure calculation of **2** (*a*) Face-on and (*b*) edge-on views; *cis*-**3** (*c*) Face-on and (*d*) edge-on views; deprotonation of *cis*-**3** (*e*) Face-on and (*f*) edge-on views.

6. UV-vis titration of *cis*-3 with F^- and selective testing in CH_3CN

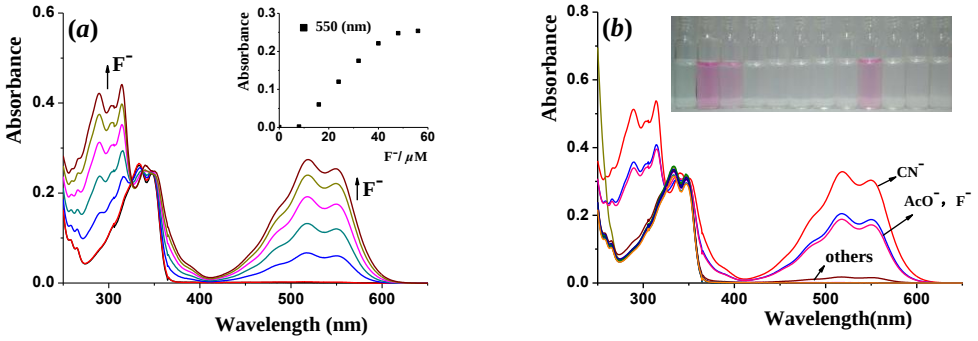

Figure S23. (*a*) UV-visible titration of *cis*-**3** (20 μM) with TBAF (0 to 2.7 equiv.) in CH_3CN. The inset shows the absorbance at 550 nm as a function of [F^-]; (*b*) UV-visible spectra of *cis*-**3** (20 μM) in the presence of different anions (ca.1.6 equiv) in CH_3CN; Inset: Color change of *cis*-**3** with different anions (from left to right: *cis*-**3** only, CN^-, F^-, Cl^-, Br^-, I^-, HSO_4^-, $H_2PO_4^-$, AcO^-, BF_4^-, NO_3^-, ClO_4^-).

7. UV-vis interference experiments of *cis*-3 toward CN^- in CH_3CN and CH_3CN-H_2O

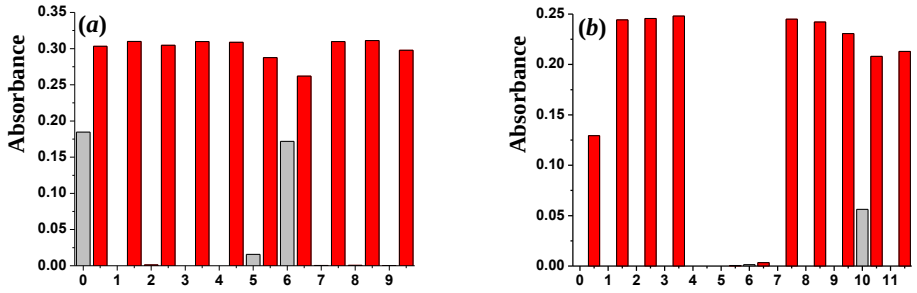

Figure S24. (*a*) Interference experiments of *cis*-**3** (20 μM) in CH_3CN for CN^- in the presence of other anions. The gray bars represent the emission at 550 nm of *cis*-**3** in the presence of 1.6 equiv. of the anion of interest (from 0 to 9: F^-, Cl^-, Br^-, I^-, HSO_4^-, $H_2PO_4^-$, AcO^-, BF_4^-, NO_3^-, ClO_4^-). The red bars indicate the change that occurs upon subsequent addition of 1.6 equiv. of CN^- to the solution containing *cis*-**3** and the anion of interest; (*b*) Interference experiments of *cis*-**3** (20 μM) in CH_3CN/H_2O (9:1, v/v) for CN^- in the presence of other anions. The gray bars represent the emission at 545 nm of *cis*-**3** in the presence of 80.0 equiv. of the anion of interest (from 0 to 9: F^-, Cl^-, Br^-, I^-, HSO_4^-, $H_2PO_4^-$, AcO^-, BF_4^-, NO_3^-, ClO_4^- , S^{2-}, SCN^-). The red bars indicate the change that occurs upon subsequent addition of 80.0 equiv. of CN^- to the solution containing *cis*-**3** and the anion of interest.

8. Influence of pH on the absorbance of *cis*-3 in CH_3CN-H_2O

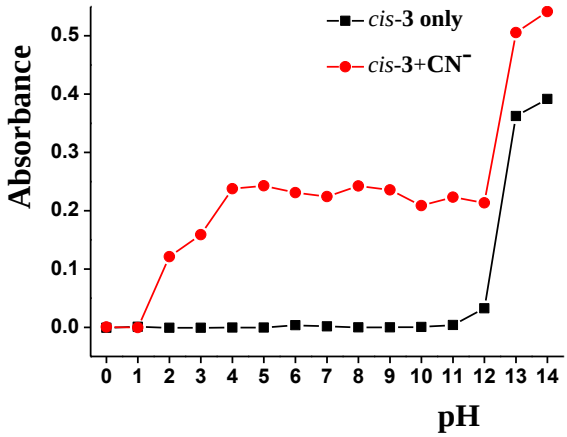

Figure S25. Influence of pH on the absorbance at 550 nm of *cis*-**3** and *cis*-**3**+CN^- in CH_3CN/H_2O (9:1, v/v).

9. Emission spectra of titration of *cis*-3 with CN^- and selective testing in CH_3CN

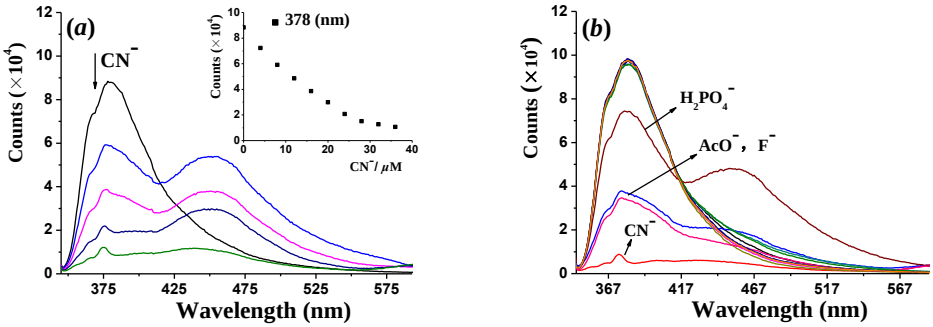

Figure S26. (*a*) Emission spectra of *cis*-**3** (20 μM, λ_{ex} = 337 nm, in CH_3CN) upon addition of increasing concentrations of CN^- (as its TBA salt, 0 to 1.8 equiv). Inset: Plot of emission intensity (λ_{em} =378 nm) versus TBACN concentration; (*b*) Fluorescence spectra of *cis*-**3** (20 μM) in the presence of different anions (CN^-, F^-, Cl^-, Br^-, I^-, HSO_4^-, $H_2PO_4^-$, AcO^-, BF_4^-, NO_3^-, ClO_4^-) (ca. 1.8 equiv.) in CH_3CN.

10. Emission interference experiments of *cis*-3 toward CN^- in CH_3CN and CH_3CN-H_2O

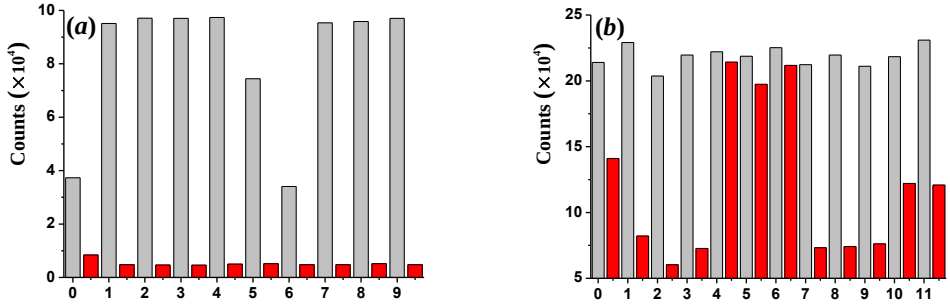

Figure S27. (*a*) Fluorescence spectra of probe *cis*-**3** (20 μM) in presence of various anion (1.8 equiv.) in CH_3CN solution. The gray bars represent the emission at 378 nm in the presence of 1.8 equiv. of the anion of interest (form 0 to 9: F^-, Cl^-, Br^-, I^-, HSO_4^-, $H_2PO_4^-$, AcO^-, BF_4^-, NO_3^-, ClO_4^-). The red bars indicate the change that occurs upon subsequent addition of 1.8 equiv. of CN^- to the solution containing *cis*-**3** and the anion of interest; (*b*) Fluorescence spectra of probe *cis*-**3** (20 μM) in presence of various anion (90.0 equiv.) in CH_3CN solution. The gray bars represent the emission at 388 nm in the presence of 90.0 equiv. of the anion of interest (form 0 to 11: F^-, Cl^-, Br^-, I^-, HSO_4^-, $H_2PO_4^-$, AcO^-, BF_4^-, NO_3^-, ClO_4^-, S^{2-}, SCN^-). The red bars indicate the change that occurs upon subsequent addition of 90.0 equiv. of CN^- to the solution containing *cis*-**3** and the anion of interest.

11. The fluorescence detection limit of *cis*-3 with CN^- in CH_3CN-H_2O solution.

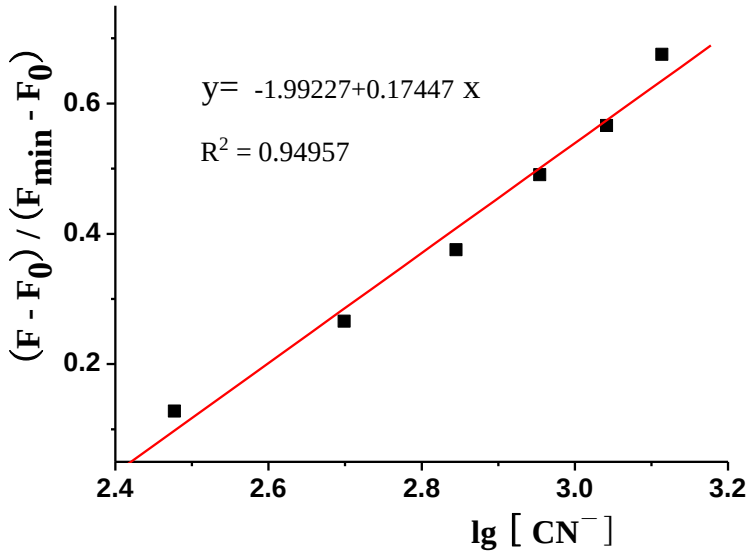

Figure S28. Emission intensity ratio (F_{488}) of *cis*-**3** (20 μM) as a function of CN^- concentration from 0-1800 μM (0–90 equiv) in in CH_3CN/H_2O (9:1, v/v).

Equiation	Y = A + B * X	
Parameter	Value	Error
A	-1.99227	0.84379
B	0.17447	0.06093
R	SD	N

0.97446	0.03218	9

The result of the analysis as follows:

Linear Equation: Y = -1.99227+0.17447* X, R^2 = 0.94957

S= 0.17447 * 10^6, K = 3, δ = 0.0.03218

LOD = K *δ / S = 0.553 μM

12. Molecular modeling calculations for *trans*-3

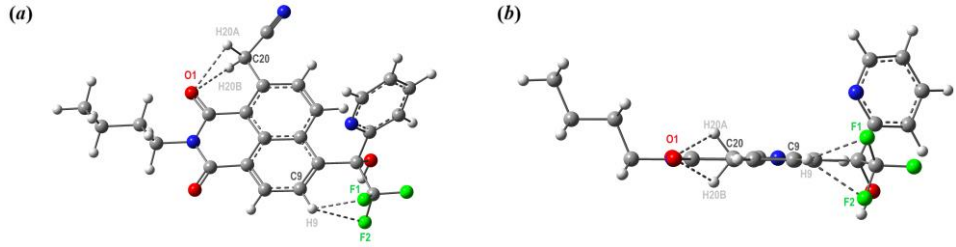

	Bond lengths				angles			
	H9-F1	H9-F2	O2/O1-H20A	O2/O1-H20B	C9-H9-F1	C9-H9-F2	C20-H20A-O2	C20-H20B-O2
trans-**3**	2.26034	2.44762	2.38258	2.38806	118.72137	108.25962	92.60166	92.30756

Figure S29. Equilibrium structure calculation of *trans*-**3** (*a*) Face-on and (*b*) edge-on views.

13. UV-vis absorbance spectra of *trans*-3

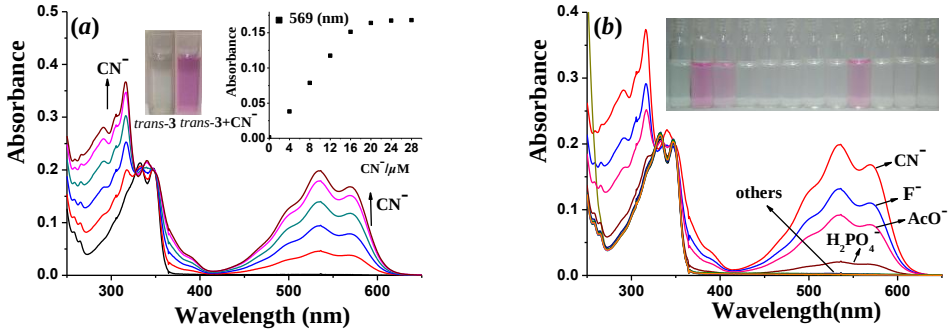

Figure S30. (*a*) UV-visible titration of *trans*-**3** (20 μM) with TBACN (0 to 1.2 equiv.) in CH_3CN. The inset shows the absorbance at 569 nm as a function of CN^-; (*b*) UV-visible spectra of *trans*-**3** (20 μM) in the presence of different anions (ca.1.2 equiv) in CH_3CN; Inset: Color change of *trans*-**3** with different anions (from left to right: *trans*-**3** only, CN^-, F^-, Cl^-, Br^-, I^-, HSO_4^-, $H_2PO_4^-$, AcO^-, BF_4^-, NO_3^-, ClO_4^-).

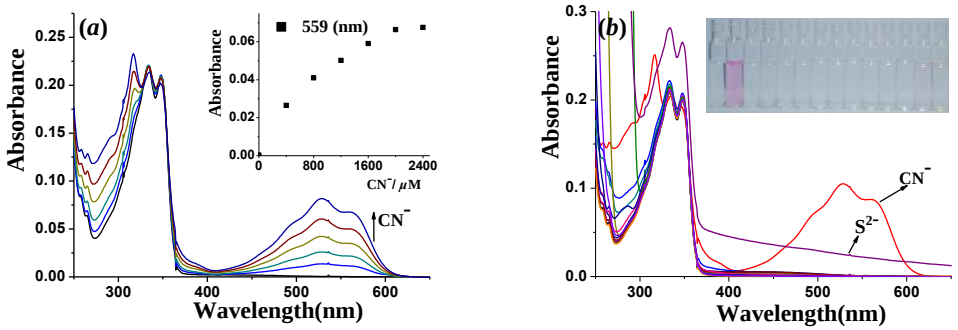

Figure S31. (*a*) UV-visible titration of *trans*-**3** (20 μM) with TBACN (0 to 100.0 equiv.) in CH_3CN/H_2O (9:1, v/v). The inset shows the absorbance at 559 nm as a function of CN^-; (*b*) UV-visible spectra of *trans*-**3** (20 μM) in the presence of different anions (ca.100.0 equiv) in CH_3CN/H_2O (9:1, v/v); Inset: Color change of *trans*-**3** with different anions (from left to right: *trans*-**3** only, CN^-, F^-, Cl^-, Br^-, I^-, HSO_4^-, $H_2PO_4^-$, AcO^-, BF_4^-, NO_3^-, ClO_4^- , S^{2-}, SCN^-).

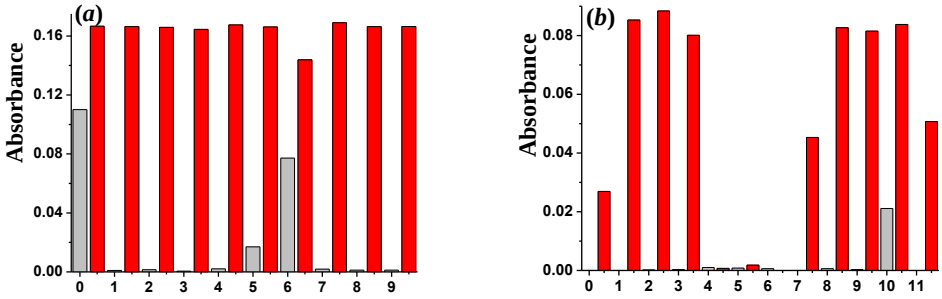

Figure S32. (*a*) Interference experiments of *trans*-**3** (20 μM) in CH_3CN for CN^- in the presence of other anions. The gray bars represent the emission at 569 nm of *trans*-**3** in the presence of 1.2 equiv. of the anion of interest (from 0 to 9: F^-, Cl^-, Br^-, I^-, HSO_4^-, $H_2PO_4^-$, AcO^-, BF_4^-, NO_3^-, ClO_4^-). The red bars indicate the change that occurs upon subsequent addition of 1.2 equiv. of CN^- to the solution containing *trans*-**3** and the anion of interest; (*b*) Interference experiments of *trans*-**3** (20 μM) in CH_3CN/H_2O (9:1, v/v) for CN^- in the presence of other anions. The gray bars represent the emission at 559 nm of *trans*-**3** in the presence of 100.0 equiv. of the anion of interest (from 0 to 9: F^-, Cl^-, Br^-, I^-, HSO_4^-, $H_2PO_4^-$, AcO^-, BF_4^-, NO_3^-, ClO_4^- , S^{2-}, SCN^-). The red bars indicate the change that occurs upon subsequent addition of 100.0 equiv. of CN^- to the solution containing *trans*-**3** and the anion of interest.

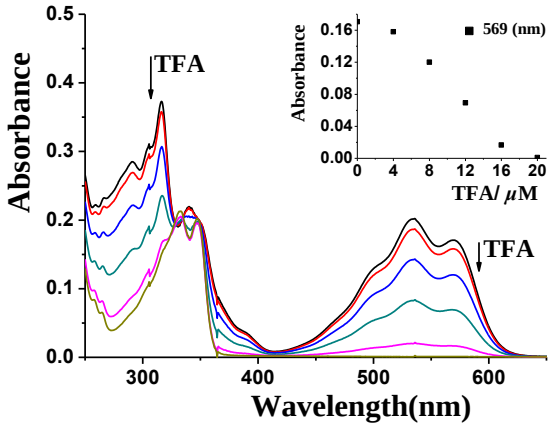

Figure S33. UV-visible titration of *trans*-**3**+CN^- (20 μM) with TFA (0 to 1.2 equiv.) in CH_3CN. The inset shows the absorbance at 569 nm as a function of TFA.

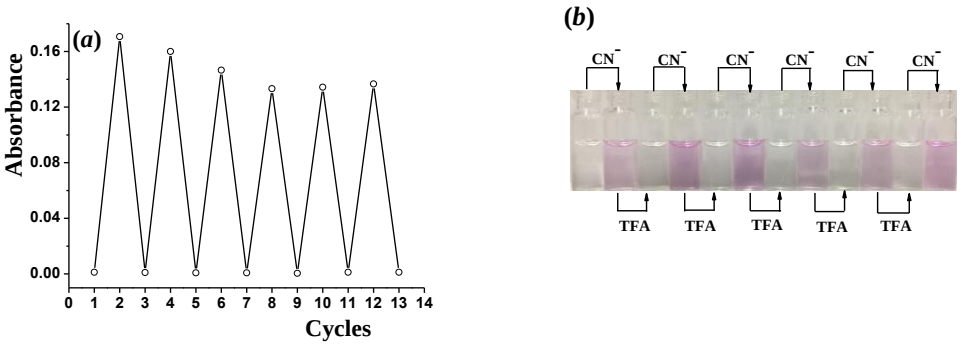

Figure S34. (*a*) Relative UV-visible absorbance during the titration of *trans*-**3** with CN^- and H^+ (TFA) in CH_3CN; (*b*) visual color after each sequential addition of CN^- and H^+ (TFA) in CH_3CN.

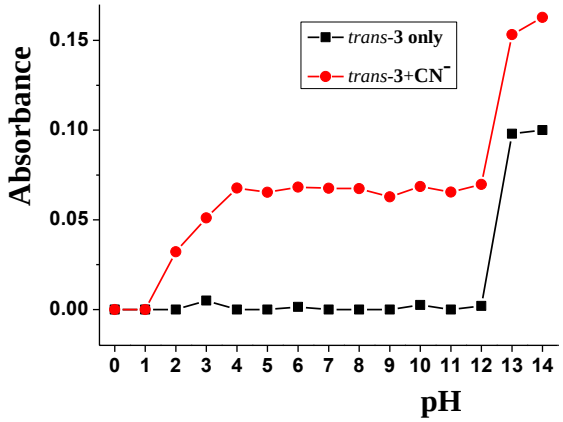

Figure S35. Influence of pH on the absorbance at 559 nm of *trans*-**3** and *trans*-**3**+CN^- in CH_3CN/H_2O (9:1, v/v).

14. Fluorescence emission spectra of *trans*-3

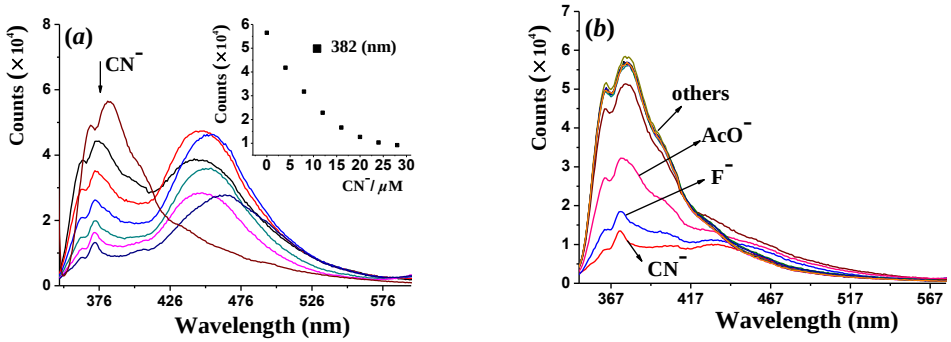

Figure S36. (*a*) Emission spectra of *trans*-**3** (20 μM, λ_{ex} = 335 nm, in CH_3CN) upon addition of increasing concentrations of CN^- (as its TBA salt, 0 to 1.4 equiv). Inset: Plot of emission intensity (λ_{em} =382 nm) versus TBACN concentration; (*b*) Fluorescence spectra of *trans*-**3** (20 μM) in the presence of different anions (CN^-, F^-, Cl^-, Br^-, I^-, HSO_4^-, $H_2PO_4^-$, AcO^-, BF_4^-, NO_3^-, ClO_4^-) (ca. 1.4 equiv.) in CH_3CN.

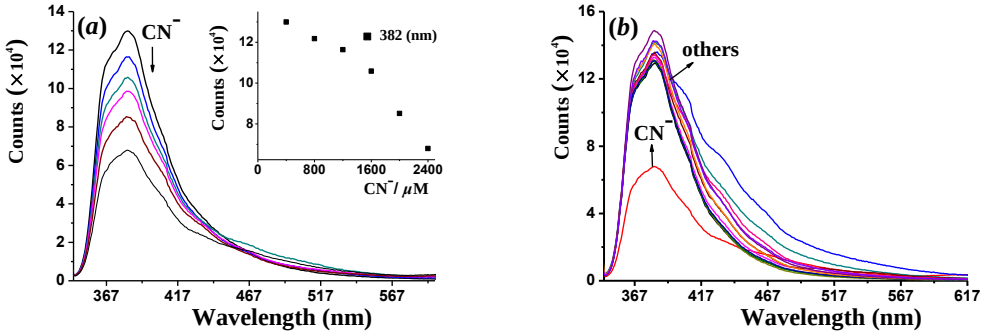

Figure S37. (*a*) Emission spectra of *trans*-**3** (20 μM, λ_{ex} =335 nm, in CH_3CN/H_2O (9:1, v/v)) upon addition of increasing concentrations of CN^- (as its TBA salt, 0 to 120.0 equiv). Inset: Plot of emission intensity (λ_{em} = 382 nm) versus TBACN concentration; (*b*) Fluorescence spectra of *trans*-**3** (20 μM) in the presence of different anions (CN^-, F^-, Cl^-, Br^-, I^-, HSO_4^-, $H_2PO_4^-$, AcO^-, BF_4^-, NO_3^-, ClO_4^-, S^{2-}, SCN^-) (ca. 120.0 equiv) in CH_3CN/H_2O (9:1, v/v).

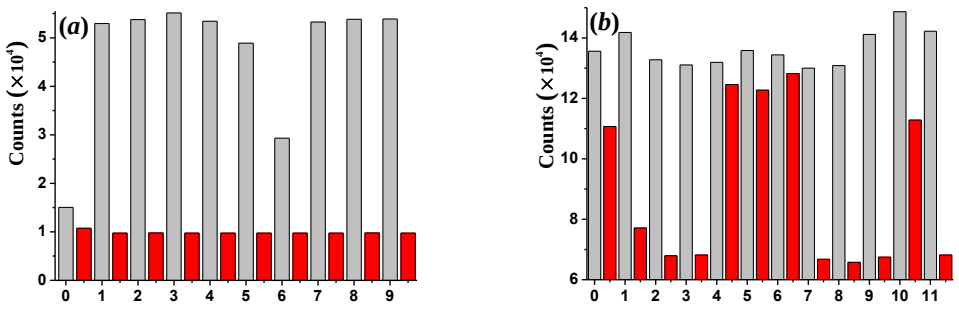

Figure S38. (*a*) Fluorescence spectra of probe *trans*-**3** (20 μM) in presence of various anion (1.4 equiv.) in CH_3CN solution. The gray bars represent the emission at 382 nm in the presence of 1.4 equiv. of the anion of interest (form 0 to 9: F^-, Cl^-, Br^-, I^-, HSO_4^-, $H_2PO_4^-$, AcO^-, BF_4^-, NO_3^-, ClO_4^-). The red bars indicate the change that occurs upon subsequent addition of 1.4 equiv. of CN^- to the solution containing *trans*-**3** and the anion of interest; (*b*) Fluorescence spectra of probe *trans*-**3** (20 μM) in presence of various anion (120.0 equiv.) in CH_3CN/H_2O (9:1, v/v) solution. The gray bars represent the emission at 382 nm in the presence of 120.0 equiv. of the anion of interest (form 0 to 11: F^-, Cl^-, Br^-, I^-, HSO_4^-, $H_2PO_4^-$, AcO^-, BF_4^-, NO_3^-, ClO_4^-, S^{2-}, SCN^-). The red bars indicate the change that occurs upon subsequent addition of 120.0 equiv. of CN^- to the solution containing *trans*-**3** and the anion of interest.